

---

# *de novo* GENE BIRTH AS AN INEVITABLE CONSEQUENCE OF ADAPTIVE EVOLUTION

---

**Somya Mani and Tsvi Tlusty**  
Center for Soft and Living Matter - Institute for Basic Science  
Ulsan 44919, Republic of Korea  
somyamn@gmail.com; tsvitlusty@gmail.com

May 20, 2022

## ABSTRACT

Phylostratigraphy suggests that new genes are continually born *de novo* from non-genic sequences. The genes that persist found new lineages, contributing to the adaptive evolution of organisms. While recent evidence supports the view that *de novo* gene birth is frequent and widespread, the mechanisms underlying this process are yet to be discovered. Here we hypothesize and examine a potential general mechanism of gene birth driven by the accumulation of beneficial mutations at non-genic loci. To demonstrate this possibility, we model this mechanism, within the boundaries set by current knowledge on mutation effects. Estimates from this simple analysis are in line with observations of recurrent and extensive gene birth in genomics studies. Thus, we propose that rather than being inactive and silent, non-genic regions are likely to be dynamic storehouses of potential genes.

## 1 Introduction

Genes are sequences in the genome which yield phenotypic traits through regulatory interactions of their products with other genes and the environment [1]. Until recently, it was believed that a basic set of ‘founder genes’, numbering some thousands, evolved a long time ago, and all new genes are exclusively derived from these founder genes. In contrast to this ‘genes come from genes’ picture, genomic evidence indicates that 10–30% of all genes across eukaryotic genomes are orphan genes, for which no homology can be detected with any established, conserved genes [2]. While it is possible that orphan genes are products of duplication and rapid divergence of conserved genes, recent studies indicate that most orphan genes are likely to be generated *de novo* starting from previously non-genic sequences [3]. Moreover, phylostratigraphy suggests that such new genes are generated continuously [2].

Known *de novo* genes display some intriguing patterns: new genes are born preferably in genomic regions with high GC content and near meiotic hot spots. In animals, new genes are more likely to be expressed in the brain and testis [4]. Interestingly, these cells and genomic regions are also especially prone to pervasive transcription [5]. These observations point to a possible mechanism of gene birth [6], whereby non-genic loci, made visible to natural selection by pervasive expression, can be driven to evolve in two ways: the sequences could evolve towards reducing deleterious traits, such as propensity to aggregate, in a process called pre-adaptation [7, 8]; alternatively, or additionally, the sequences can gain new functions that increase the fitness of the organism [9]. Pre-adaptation is considered non-adaptive evolution since it ensures that expressed sequences remain harmless, but in itself does not prescribe how the expression of these sequences increase organismal fitness. Whereas gain of a new function is considered adaptive and leads to gene birth.

Furthermore, two simple studies, taken together, lend support to such a mechanism of gene birth: first, random sequences can gain functionality, provided they are consistently expressed [10]. And second, it was demonstrated that new promoters could easily evolve in *E. coli* [11]. These studies highlight the possibility that non-genic sequences can, in stages, gain the hallmarks of genes: regulated expression and functionality.

Here we hypothesize that gene birth can be understood as an inevitable consequence of adaptive evolution of non-genic sequences. To demonstrate this, we present a blueprint for a minimal model of gene birth that uses characteristics of spontaneous mutations, the simplest units of adaptive evolution, as its building blocks. Specifically, we consider the

process by which a locus that initially provides very low fitness advantage, corresponding to leaky expression, starts to accumulate beneficial mutations. We conjecture that this process reflects the early stages of *de novo* gene birth.

Fitness effects of spontaneous mutations are assessed experimentally through mutation accumulation studies. These studies directly [12], or indirectly [13] allow inference of the fitness effects of single mutations, thereby yielding a distribution of fitness effects (DFE). The DFE is known to differ across different regions of the genome [14], and across different species [15]. We accommodate this diversity by sampling a wide range of DFEs, which differ in the frequency and size of beneficial mutations, and also in the shape of the distribution, to assess the conditions under which spontaneous mutations can lead to gene birth.

Although functionality and regulated expression are essential features of a gene, there is a dearth of quantitative data that describes the evolution of these features. Therefore, we use a very coarse-grained definition of genes, which is free from considerations of what its exact function is or the mechanism through which the gene achieves its function, which allows us to leverage currently available data to produce biologically reasonable estimates.

Our model indicates that gene birth should be highly likely for a wide range of DFEs, given a time frame of millions of years. Especially, we find that the presence of rare, large-effect mutations can potentially compensate for beneficial mutations being small and infrequent on average. We also tested the more realistic scenario where the DFE of a genomic locus fluctuates over the long periods of time; under these conditions, gene birth becomes practically inevitable.

Based on this simple analysis, we propose the intriguing hypothesis that *de novo* gene birth through the adaptive evolution of non-genic sequences is practically unavoidable. We also discuss experiments to test some consequences of this hypothesis. We anticipate that in the future, experiments would characterize not only the fitness effects of mutations, but also distinguish between their effect on expression level of loci and functionality of expression products. Such data should inform more detailed models that capture the essence of genes, and therefore of the process of *de novo* gene birth.

## 2 An adaptive model of gene birth

We use the Wright-Fischer framework to model well-mixed populations of fixed size  $N$ , composed of asexually reproducing haploid individuals. For each individual  $i$ , we consider the fitness contribution  $F_i$  of a single locus in its genome. Here, fitness represents exponential growth rate, which is equivalent to the quantities considered in experiments that measured DFEs (e.g., [13]).

Genes can be defined at many levels; currently, it is customary to associate a gene with the sequence of a genomic locus that is conserved and produces a functional product. Genes can also be described in terms of the products they specify and the molecular interactions of these products. Here, we use a coarse-grained description of a gene and define it using its fitness contribution to the organism, and the DFE of its locus in the genome. Although our definition of genes is minimal, it includes two salient features of genes: *heritability* of the fitness level, and its *mutability*. In the model, since our definition of the gene is not tied to any specific function, we describe a locus as *genic* if it consistently contributes a fitness advantage above a predetermined *genic threshold* and non-genic otherwise.

The standard Wright-Fischer model is traditionally used to study the evolution of genes; here we apply the model to non-genic loci and test the predictions it makes for *de novo* gene birth. Initially, the locus of interest is non-genic, and the distribution of  $F_i$  is centered around 0 and any small fitness effect is due to leaky expression. In each subsequent time-step  $t + 1$ , the population is composed entirely of the offspring of individuals in the current time-step  $t$  (Fig.1(A)). The probability that an individual leaves an offspring is proportional to the fitness  $F_i$  of the locus, and individuals with  $F_i \leq -1$  cannot produce offspring. Additionally, offspring in the model incur mutations. This sets the timescale of the model according to the mutation rate of the organism: a time-step in the model is roughly the time it takes for a mutation to occur in the locus. For a locus of  $\sim 100$  base pairs, a single model time-step can range between 100–100,000 years for different organisms (Fig.1(B), see also Fig.1–Figure Supplement1).

The fitness effects of mutations are drawn from the characteristic DFE for the locus (Fig.1(C)). Multiple studies indicate that long-tails are important features of DFEs, and the gamma distribution is a general form which can describe such long-tailed distributions [16]. Therefore, we choose to follow [13], and represent DFEs as two-sided gamma distributions, and characterize them using four parameters: (i) average effect of beneficial mutations  $p$ , (ii) fraction of beneficial mutations  $f$ , (iii) average effect of deleterious mutations  $n$ , and (iv) the shape parameter  $s$ , where distributions with lower shape parameters are more long-tailed. Note that, although experimental studies report DFEs across the whole genome, here we assume that the characteristics of the DFE of single loci are similar. The mutation types we deal with in the model are those that were included in [13], which were single-nucleotide mutations and short indels (on average  $\leq 10$  bp) [17]. We account for differences in DFEs across species and locations on the genome by sampling

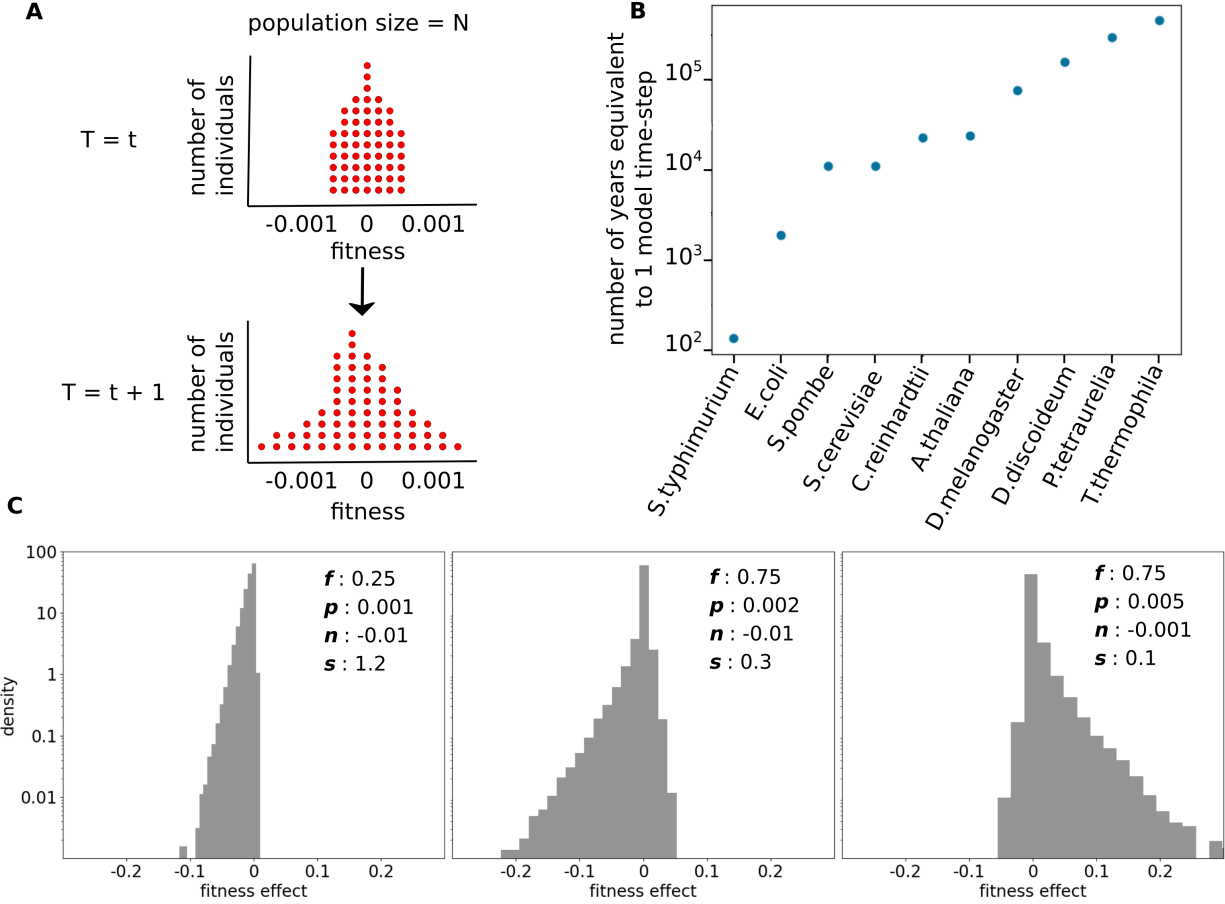


**Figure 1: Time-scale and fitness effects of mutations in the model.** (A) Model schematic. Each red dot represents the fitness contribution of the locus of interest in an individual of the population. At some time step  $T = t + 1$ , the population is replaced by offspring of the previous population at  $T = t$ . The fitness of an offspring depends on the fitness of its parent and the effect of any mutation incurred. (B) Estimates of the number of years equivalent to a single time-step of the model in the different species listed on the x-axis. See Fig1–Figure Supplement1 for calculations. (C) DFE for different model parameters. The left panel represents the DFE with the most deleterious and least beneficial mutations. The right panel represents the DFE with the most beneficial and least deleterious mutations sampled in this work. The center panel represents the DFE with parameters closest to those reported in [13]. Values of parameters used to construct these DFEs are given alongside each histogram.

across biologically reasonable values of these four parameters  $p, f, n, s$  (see Surveying the space of DFEs in populations of various sizes). In all, we survey 225 parameter sets, and run 100 replicate populations for each set of DFE parameters.

We update populations for 2,500 time-steps, equivalent to 0.2–200 million years, depending on the organism (see Method to update population fitness for finite populations). In finite populations, we can trace the ancestry of each locus in each individual (see Tracing ancestry and finding the fitness of the fixed mutation), which allows us to track *fixation events*: a mutant is said to have *fixed* in the population if the ancestry of all individuals at some time-step  $t$  can be traced back to a single individual at some previous time-step  $t - t_{\text{fix}}$ . During the course of a simulation, populations undergo multiple fixation events. We say that *de novo* gene birth occurs when the most recent mutant that gets fixed in the population is fitter than the predetermined *genic* threshold. For infinite populations, we model the evolution of the locus as a stochastic process (see Method to update population fitness for infinite populations). In this case, we say that gene birth occurs when the average fitness of the population is greater than the *genic* threshold.

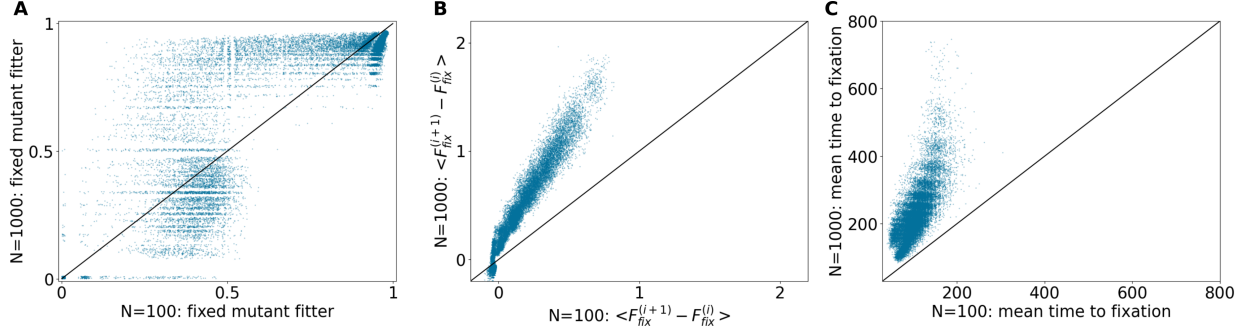


**Figure 2: Scatter plots comparing fixation dynamics in  $N = 100$  and 1,000 populations.** For each population size, 22,500 systems were analysed across all parameter values. For each point, the x-coordinate represents an  $N = 100$  and the y-coordinate represents an  $N = 1,000$  population that have the same parameter values. (A) Fraction of times fixation of fitter mutant occurred, (B) mean fitness difference between current and previous fixed mutant,  $\langle \Delta F_{\text{fix}} \rangle = \langle F_{\text{fix}}^{i+1} - F_{\text{fix}}^i \rangle$ , where  $F_{\text{fix}}^i$  is the fitness of the  $i^{\text{th}}$  mutant that fixed in the population, and (C) mean fixation time across 2,500 time steps. See Fig2–Figure Supplement1 for scatter plots comparing  $N = 1,000$  and 5,000.

### 3 Predictions from the adaptive model

#### 3.1 Small populations fix fewer beneficial mutations faster

In our model, we look at fixation dynamics in populations of size  $N = 100, 1,000$  and 5,000. It is well-known in population dynamics that small populations are generally subject to stronger genetic drift, which makes it harder for fitter mutants to fix ([18], chapter 2). Additionally, mathematical models of the Moran process indicate that fitter mutants have a lower fixation probability and a shorter fixation time in smaller populations [19]. Consistently, we find that the probability of fixation of fitter *de novo* mutants that arise in smaller populations is lower (Fig.2(A), Table.1(row1), Fig2–Figure Supplement1(A)). Moreover, across all fixation events, the mean fitness difference between the current fixed mutation and the previously fixed mutation tends to be much higher in larger populations (Fig.2(B), Fig2–Figure Supplement1(B)). And fixation occurs much faster in  $N = 100$  populations (Fig.2(C), Table.1(row2), Fig2–Figure Supplement1(C)).

**Table 1: Dynamics of fixation of beneficial mutations in finite populations.** (Row1) The fraction of systems in which a fitter mutant fixed in the population at least 75% of the time across 2,500 time-steps. (Row2) The average of mean-fixation time across 2,500 time-steps.

	N=100	N=1000	N=5000
Fraction of systems where a fitter mutant fixed at least 75 % of the time	0.57	0.70	0.77
Mean time-steps to fixation	104.2	226.2	296.4

#### 3.2 Most parameters allow gene birth

Surprisingly, a majority of parameters in our survey are conducive to gene birth (Fig.3(A)). This finding suggests that gene birth due to spontaneous mutations should be a universal process, and we should expect it to occur in a wide variety of organisms and across many distinct genomic regions. The rate of gene birth should scale according to features of the organisms such as its generation time and mutation rate (Fig.1(B), Fig1–Figure Supplement1). As expected, gene birth is more prevalent in larger populations (Table.2(row1)). All parameters that allow gene birth in a small population also allow it in larger populations. Although the number of permissive parameters decreases as the genic threshold is increased, the results remain qualitatively the same (Fig3–Figure Supplement1). Also, as expected from fixation time distributions for finite populations, when gene birth occurred, it was faster in smaller populations (Table.2(row2), Fig.4, Fig3–Figure Supplement1).

**Table 2: Dynamics of gene birth for a genic threshold of 0.1.** (Row1) The fraction of parameters out of 225 in which gene birth was observed. For finite populations, this is the number of parameters where gene birth occurred in at least one out of 100 replicate populations. (Row2) Average time to gene birth.

	N=100	N=1000	N= $\infty$
Parameters with observed gene birth	68.0%	76.9%	96.4%
Mean time-steps to gene birth	380.7	452.4	357.7

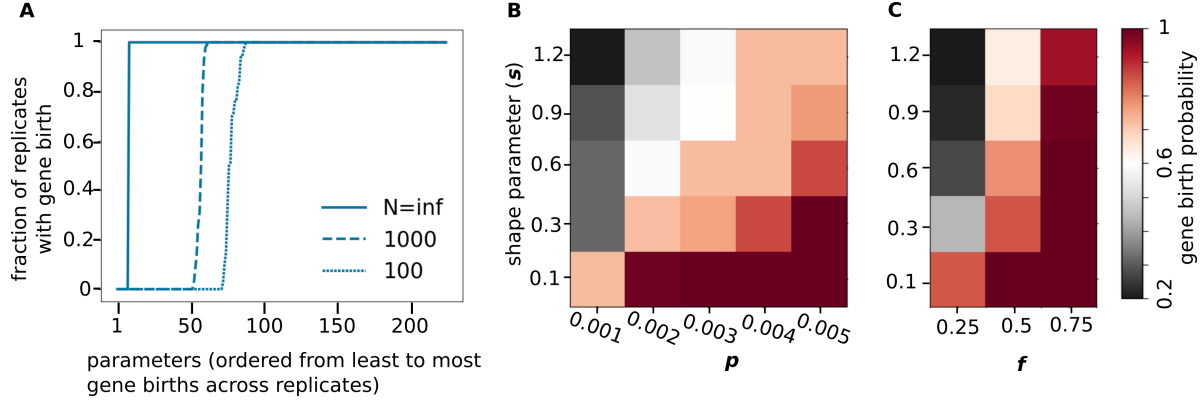


**Figure 3: Probability of gene birth.** (A) The fraction of replicate systems at different parameter values that achieve gene birth. See also Fig3–Figure Supplement1. (B,C) Trade-off between the shape parameter,  $s$  (B) size of beneficial mutations,  $p$  and (C) the frequency of beneficial mutations,  $f$ . We show results here for populations of size  $N = 1,000$ . See Fig3–Figure Supplement2 for  $N = 100, \infty$ . In the heatmaps, rows indicate values of the shape parameter and columns indicate values of parameters  $p$  and  $f$ , respectively. Colors indicate the fractions of systems with gene birth as shown in the colorbar. See Fig3–Figure Supplement3 for effect of parameters on gene birth probability in populations of different sizes.

### 3.3 Rare large-effect beneficial mutations are sufficient for gene birth

Across all population sizes, gene birth is more likely when the frequency  $f$  and average size  $p$  of beneficial mutations are higher, the size of deleterious mutations  $n$  is lower, and the DFE is more long-tailed (Fig3–Figure Supplement3). Although gene birth depends strongly on beneficial mutations, we find that it can still occur in populations with small values of parameters  $f$  and  $p$ , provided the DFE of mutations is long-tailed (i.e., small values of  $s$ ) (Fig.3(B,C), see also Fig3–Figure Supplement2). This suggests that large-effect beneficial mutations are sufficient for gene birth, even when they are rare.

### 3.4 Gene birth is practically inevitable under DFE fluctuations

The DFE of a genomic locus is likely to change over time. In addition to sampling across different parameters, we also test how fluctuations in the DFE could effect gene birth. Broadly, there are three ways in which the DFE shifts in nature:

- Over relatively short periods of time, under fairly constant environments, organisms experience ‘diminishing returns epistasis’, whereby the fitness gains due to beneficial mutations are smaller in relatively fit individuals than unfit individuals. Therefore, diminishing returns epistasis is likely to lead to decreased fitness gains along adaptive trajectories [20]. In terms of the model, this would look like the DFE parameter  $p$  reducing over time as fitter mutants undergo fixation in populations.
- Over longer periods, environmental changes could lead to DFE variations due to changes in the magnitude of mutation effects, maybe even switching the sign of some mutations from beneficial to deleterious and vice-versa [21].
- The DFE can also change because of changes in frequencies of different types of mutations, such as transitions or transversions. This can happen when there is a shift in mutational biases, such as in mutator strains in *E. coli* [12].

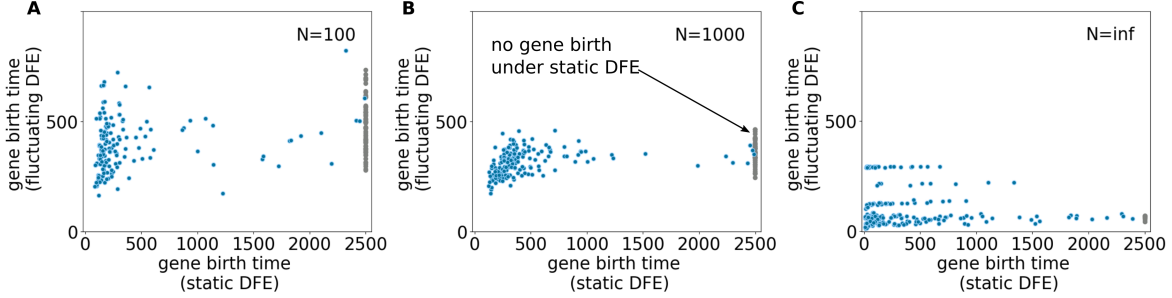


**Figure 4: Scatter plots comparing gene birth time in systems with static vs. fluctuating DFE.** For each point, the parameters for the static DFE and the initial parameters for fluctuating DFE are the same. The x-axis represents average time of gene birth across 100 replicate systems with static DFE, and the y-axis represents the average time of gene birth across 10 replicate systems when the DFE fluctuates, for (A)  $N = 100$ , (B)  $N = 1,000$ , and (C)  $N = \infty$ . The grey points that accumulate at  $x = 2,500$  represent parameter values at which gene birth did not occur in static DFE systems. See also Fig4–Figure Supplement1,2,3

Since the time-scale of each step in our model is of the order of hundreds to thousands of years, we do not expect diminishing returns epistasis to persistently affect gene birth. And environmental changes are expected to change not only the DFE of new mutations, but also fitness contributions of preexisting genes, which is beyond the scope of the current model. Thus, the fluctuations we test in the model best represent shifts in mutational biases, which are expected to only affect the DFE of new mutations. This is modelled by allowing one of the parameters of the DFE to shift to a neighbouring value at each time-step. For each initial parameter set, we run 10 replicate populations. While shifts in mutational bias are predicted to increase beneficial mutations [12], we also allow fluctuations that decrease beneficial mutations; these could represent a depletion of easily accessible beneficial mutations when the same mutational bias operates over long periods.

We find that allowing DFE parameters to fluctuate makes gene birth almost inevitable in systems of all population sizes tested, and regardless of initial parameters. In Fig.4 (A,B,C), the grey points represent parameter values that did not lead to gene birth in any replicate population with static DFE. But under fluctuating DFE, gene birth occurs in all populations. For a large proportion of parameters, gene birth was faster, and gene birth times fall in a narrow range under fluctuating DFE (Fig.4, see also Fig4–Figure Supplement1). To understand this high probability of gene birth under this scheme of DFE fluctuations, we notice that although each time-step involves only a small change in DFE parameters, almost all parameter sets are visited at least once over 2,500 time-steps, irrespective of initial parameters (Fig4–Figure Supplement2,3). Now, across  $N = 100$ , 1,000 populations, 60.9% and 72.4%, respectively, of all parameters led to gene birth in all 100 replicate systems (Fig.3(A)). And, on average, these are the fractions of time steps along the 2,500 time-step trajectory in which the fluctuating systems visited these high gene birth parameters. This indicates that this scheme of DFE fluctuations uniformly samples all available DFEs over long enough periods of time. The substantial time spent in highly permissive parameters explains the high incidence of gene birth. It also implies that these systems are effectively equivalent irrespective of initial parameter values, thus explaining the narrow distribution of time to gene birth. That is, gene birth depends on the duration a population spends in conditions conducive to gene birth, and is robust to the history of succession of these conditions. Altogether, this bolsters the view that *de novo* gene birth is a widespread process.

## 4 Discussion

The study of *de novo* genes draws attention to problems with our very conception of what a gene is [1]. It appears that organisms adapt not only by optimizing preexisting genetic modules to environmental parameters, but also through the invention of new genes, which exist transiently [22]. How often genes are born *de novo*, the time-scale of gene birth, and the time for which they persist, are therefore important questions that are fundamental to our understanding of adaptive evolution.

We explore here a simple mathematical model to study aspects of *de novo* gene birth. Principally, we investigate the probability and the expected time frame of gene birth under various conditions. Our conception of a ‘gene’ is coarse-grained, representing the gene only by its adaptive value. For instance, birth of specific classes of genes, such as anti-freeze proteins [23] or miRNA [24], might display very different dynamics. Specifically, the emergence of function in *de novo* genes that express proteins is very likely linked to the evolution of structural features [25], but our model is agnostic to the molecular mechanisms by which functionality is achieved. Our approach is therefore immensely simple,

but it comes with trade-offs; importantly, this framework cannot capture non-adaptive aspects of genome evolution. For example, we cannot test here the role of pre-adaptation, which is a non-adaptive process that leads to sequences evolving away from highly deleterious phenotypes, but does not prescribe whether and how sequences gain new functions [7]. Nevertheless, an advantage of the present framework is the multitude of experimental studies that measure organismal fitness in terms of an easily accessible, universal quantity: the relative growth rate. Numerous studies measure the effect of mutations on organismal fitness in terms of the DFE, which allows us to investigate the contribution of spontaneous mutations towards gene birth.

Here we use the DFE as a one-dimensional proxy for the huge multidimensional space that describes the properties of genomic sequences. That is, we assume that the various properties of loci where *de novo* gene birth is observed, such as high GC content, presence of bidirectional promoters, and presence of meiotic hotspots [4], all enter the system via their influence on the DFE of that genomic locus. For example, we imagine that at transcriptionally permissive genomic sequences, such as bidirectional promoters and nucleosome-free meiotic hotspots, any mutations are more likely to be expressed, and therefore are more likely to display DFE with higher values of  $p$  and  $n$  parameters. The DFE also subsumes properties of the gene interaction network since the fitness contribution of any one locus depends on the cellular context in which it is expressed [26].

Ideally, a model of gene birth would include the process of evolution of both expression level and functionality. In this sense, a limitation of currently available DFE measurements is that they do not disentangle the contributions to a mutation's fitness effect due to changes in expression level versus changes in adaptive value of the locus. Such data would yield important insights into the dynamics of gene birth. For example, the birth of the *de novo* gene *poldi* in the house mouse is attributed mostly to mutations in regulatory regions, which led to increased expression [27]. More generally, the availability of such data could help resolve whether the prevalent mode of *de novo* birth of protein-producing genes is 'expression first' (loci are pervasively expressed and evolve functional features subsequently), or 'ORF first' (loci that already possess ORFs gain expression) [28].

Our analysis give us a glimpse into the dynamics of gene birth irrespective of the exact function the new gene performs. This is useful, because it is difficult to identify *a priori* what new functions could arise in an organism, as we cannot envision what new factor in its environment the organism is next going to leverage. That is, new genes and their functions can only be identified with certainty post their establishment. But the evolutionary history of well-known *de novo* genes [23], and genomic studies that identify 'proto-genes' [29] indicate that the adaptive value of new genes is built up gradually. In this scenario, our model provides a means for independent theoretical validation of observations from genomics studies about the prevalence of *de novo* gene birth, and produces estimates for the time-scale of the emergence of new genes.

Our analysis supports the idea that *de novo* gene birth is a widespread and frequent process, and depending on the organism, the process of gene birth should take on the order of  $10^5 - 10^6$  years. Particularly, our results suggest that rare, large-effect mutations that occur in the more long-tailed DFEs play a major role in facilitating gene birth. Also, under the regime of fluctuating DFE, which represents shifts in mutational biases, the likelihood of *de novo* gene birth increases even further. While large events, such as transposition, are very likely to occur in this time frame, and are known to be associated with *de novo* gene birth [30], our results suggest that small-scale spontaneous mutations, such as substitutions and small indels on their own are capable of pushing non-genic loci towards 'genehood'.

The present results provoke a natural question: why do we not see many more *de novo* genes? While gene birth is likely to be a frequent and continuous process, the number of genes in a species is observed to remain fairly constant over long periods of time [28]. One reason for this discrepancy is that recently emerged genes with low expression levels are much more likely to die than older genes that are consistently expressed [24, 22]. A second reason is the inability of current techniques to reliably detect *de novo* genes: new genes differ from established genes in sequence properties, such as length, disordered regions etc. [6]. Therefore, computational tools that are used to identify *de novo* genes based on sequence properties learnt from established genes under-count new genes. Potentially, these discrepancies could be resolved by replacing *de novo* gene identification methods that rely solely on sequence properties by methods that measure their fitness contributions. For example in [29], the fitness contributions of a chosen set of newly emerging genes are measured under conditions of gene disruption and over-expression. And in [24], the fitness effect of ablating *de novo* genes was measured to examine how new genes die. Using such techniques and similar approaches, large-scale measurements of fitness effects of expression products can be employed to gain more insight into how *de novo* genes emerge.

## 5 Methods

### 5.1 Surveying the space of DFEs in populations of various sizes

We scan across DFEs with  $p = [0.001, 0.002, 0.003, 0.004, 0.005]$ ,  $f = [0.25, 0.5, 0.75]$ ,  $n = [0.001, 0.005, 0.01]$  and  $s = [0.1, 0.3, 0.6, 0.9, 1.2]$ . And we look at populations of sizes  $N = [100, 1000, \infty]$ . For each parameter set, we simulate 100 replicate systems with finite population sizes, and simulate once for the infinite populations. In all, we look at 45,225 systems. We additionally look at fixation dynamics for 22,500 populations of size  $N = 5,000$  (100 replicates across all parameter values). All codes used to generate and analyze data are written in Python3.6.

### 5.2 Method to update population fitness for finite populations

For a population of size  $N$ , fitness of individuals at time-step  $t$  are stored the vector  $F_t \in \mathbb{R}^{N \times 1}$ , where the fitness of some individual  $i$  is  $F_t(i)$ . Now, only individuals with fitness  $> -1$  are viable, and capable of producing progeny.

Individuals in the current population that produce progeny are chosen on the basis of their relative fitness. Let  $\text{minfit}_t$  be the minimum fitness among viable individuals in  $F_t$ .

We define  $\text{allfit}_t = \sum_j (1 + F_t(j) - \text{minfit}_t)$ , for  $j$  such that  $F_t(j) > -1$ . The normalized relative fitness of individuals is then given by  $\text{relfit}_t \in [0, 1]^{N \times 1}$ , where

$$\begin{aligned} \text{relfit}_t(i) &= \frac{1 + F_t(i) - \text{minfit}_t}{\text{allfit}_t}, & \forall i \text{ s.t. } F_t(i) > -1 \\ \text{and, relfit}_t(i) &= 0, & \forall i \text{ s.t. } F_t(i) \leq -1 \end{aligned}$$

Let  $\text{Anc}_{t+1} \in \mathbb{N}^{N \times 1}$  be the list of individuals chosen from the current time-step  $t$  to leave progeny. In other words,  $\text{Anc}_{t+1}$  is the list of ancestors of the population at time-step  $t + 1$ . We define  $\text{cumfit}_t$  as the cumulative sum of  $\text{relfit}_t$ , and  $\text{Anc}_{t+1}(i) = \min(\{j \mid \text{cumfit}_t(j) \geq U(0, 1)\})$ . Here  $U(0, 1)$  is a uniform random number between 0 and 1. This method ensures that the probability of choosing an individual is proportional to its fitness.

Progeny of the current population incur mutations. The values of fitness effects of mutations incurred by each individual at time-step  $t$  is stored in  $\text{mut}_t \in \mathbb{R}^{N \times 1}$ , where

$$\begin{aligned} \text{mut}_t(i) &= \Gamma\left(s, \frac{p}{s}\right) \iff \text{Ber}(f) > 0, \\ \text{and, mut}_t(i) &= \Gamma\left(s, \frac{n}{s}\right) \iff \text{Ber}(f) = 0. \end{aligned}$$

Here  $\Gamma(\kappa, \theta)$  represents a number drawn from the gamma distribution with shape parameter  $\kappa$  and scale parameter  $\theta$ , and  $\text{Ber}(p)$  is the Bernoulli random variable which equals 1 with probability  $p$ . The updated fitness levels of the population is then given by  $F_{t+1}(i) = F_t(\text{Anc}_{t+1}(i)) + \text{mut}_t(i)$ .

### 5.3 Tracing ancestry and finding the fitness of the fixed mutation

In order to find the fitness value of the mutant fixed in the population at time-step  $t$ , we start with the list of ancestors of individuals  $\text{Anc}_t$  at time-step  $t$ .

Let  $X_t = \{i, \forall i \in \text{Anc}_t\}$  be the set of unique ancestor identities. We then recursively find  $X_{t-n} = \{i, \forall i \in \{\text{Anc}_{t-n}(j), \forall j \in X_{t-n+1}\}\}$  as the set of unique ancestor identities for  $n = 1, 2, 3, \dots, t_0$ , where  $X_{t-t_0}$  is the first singleton set encountered. This set contains a single individual at time-step  $t - t_0 - 1$ , whose mutations are inherited by every individual at time-step  $t$ . And the fitness value of the mutant fixed in the population at time-step  $t$  is then  $F_{t-t_0-1}(i)$ , where  $i \in X_{t-t_0}$ .

### 5.4 Method to update population fitness for infinite populations

In order to look at the evolution of fitness in infinite populations, we fix a reasonable bound,  $F_{\max} \gg \text{genic-threshold}$ , on the maximum value of fitness, and use  $F_{\min} = -F_{\max}$  as the minimum value of fitness. We also discretize the fitness values into levels  $F^i$  separated by intervals of size  $\delta$ , such that  $F^{i+1} - F^i = \delta$ .

Let  $\text{mut}(i \rightarrow j)$  be the probability density of a mutation of effect size  $F^j - F^i$ , where

$$\begin{aligned} \text{mut}(i \rightarrow j) &= f \cdot \Pr \left[ \Gamma \left( \frac{p}{s}, s \right) = F^j - F^i \right], & \text{if } F^j > F^i \\ \text{mut}(i \rightarrow j) &= (1 - f) \cdot \Pr \left[ \Gamma \left( \frac{n}{s}, s \right) = F^i - F^j \right], & \text{if } F^i > F^j \end{aligned}$$

The evolution of population fitness is then described by a transition matrix  $T$ , where

$$\begin{aligned} T(i, j) &= \frac{\text{mut}(i \rightarrow j)}{\sum_{k=-F_{\max}}^{F_{\max}} \text{mut}(i \rightarrow k)}, & \text{for } F^i > -1 \\ \text{and, } T(i, j) &= 0, & \text{for } F^i \leq -1 \end{aligned}$$

Let the probability of occupancy of any fitness value  $F^j$  at time-step  $t$  be  $P_t^j$ . Here, relative fitness levels can be calculated as  $\text{relfit}^i = 1 - F^i - F_{\min}$ . Then,

$$P_{t+1}^j = \frac{\sum_{i=-F_{\max}}^{F_{\max}} (P_t^i \cdot \text{relfit}^i \cdot T(i, j))}{\sum_{i=-F_{\max}}^{F_{\max}} (P_t^i \cdot \text{relfit}^i)}.$$

## 6 Acknowledgments

This work was funded by the Institute for Basic Science, South Korea, Project Code IBS-R020-D1.

## 7 Competing interests

The authors declare that they have no competing interests.

## References

- [1] Petter Portin and Adam Wilkins. The evolving definition of the term ‘‘gene’’. *Genetics*, 205(4):1353–1364, 2017.
- [2] Diethard Tautz and Tomislav Domazet-Lošo. The evolutionary origin of orphan genes. *Nature Reviews Genetics*, 12(10):692–702, 2011.
- [3] Nikolaos Vakirlis, Anne-Ruxandra Carvunis, and Aoife McLysaght. Synteny-based analyses indicate that sequence divergence is not the main source of orphan genes. *Elife*, 9:e53500, 2020.
- [4] Nikolaos Vakirlis, Alex S Hebert, Dana A Oplente, Guillaume Achaz, Chris Todd Hittinger, Gilles Fischer, Joshua J Coon, and Ingrid Lafontaine. A molecular portrait of de novo genes in yeasts. *Molecular Biology and Evolution*, 35(3):631–645, 2018.
- [5] Torben Heick Jensen, Alain Jacquier, and Domenico Libri. Dealing with pervasive transcription. *Molecular cell*, 52(4):473–484, 2013.
- [6] Stephen Branden Van Oss and Anne-Ruxandra Carvunis. De novo gene birth. *PLoS genetics*, 15(5):e1008160, 2019.
- [7] Joanna Masel. Cryptic genetic variation is enriched for potential adaptations. *Genetics*, 172(3):1985–1991, 2006.
- [8] Benjamin A Wilson, Scott G Foy, Rafik Neme, and Joanna Masel. Young genes are highly disordered as predicted by the preadaptation hypothesis of de novo gene birth. *Nature ecology & evolution*, 1(6):1–6, 2017.
- [9] Anne-Ruxandra Carvunis, Thomas Rolland, Ilan Wapinski, Michael A Calderwood, Muhammed A Yildirim, Nicolas Simonis, Benoit Charleaux, César A Hidalgo, Justin Barbette, Balaji Santhanam, et al. Proto-genes and de novo gene birth. *Nature*, 487(7407):370–374, 2012.
- [10] Yuuki Hayashi, Hiroshi Sakata, Yoshihide Makino, Itaru Urabe, and Tetsuya Yomo. Can an arbitrary sequence evolve towards acquiring a biological function? *Journal of molecular evolution*, 56(2):162–168, 2003.
- [11] Avihu H Yona, Eric J Alm, and Jeff Gore. Random sequences rapidly evolve into de novo promoters. *Nature communications*, 9(1):1–10, 2018.
- [12] Mrudula Sane, Gaurav D Diwan, Bhoomika A Bhat, Lindi M Wahl, and Deepa Agashe. Shifts in mutation spectra enhance access to beneficial mutations. *bioRxiv*, 2020.

- [13] Katharina B Böndel, Susanne A Kraemer, Toby Samuels, Deirdre McClean, Josianne Lachapelle, Rob W Ness, Nick Colegrave, and Peter D Keightley. Inferring the distribution of fitness effects of spontaneous mutations in *chlamydomonas reinhardtii*. *PLoS biology*, 17(6):e3000192, 2019.
- [14] Fernando Racimo and Joshua G Schraiber. Approximation to the distribution of fitness effects across functional categories in human segregating polymorphisms. *PLoS Genet*, 10(11):e1004697, 2014.
- [15] Christian D Huber, Bernard Y Kim, Clare D Marsden, and Kirk E Lohmueller. Determining the factors driving selective effects of new nonsynonymous mutations. *Proceedings of the National Academy of Sciences*, 114(17):4465–4470, 2017.
- [16] Adam Eyre-Walker and Peter D Keightley. The distribution of fitness effects of new mutations. *Nature Reviews Genetics*, 8(8):610–618, 2007.
- [17] Rob W Ness, Andrew D Morgan, Radhakrishnan B Vasanthakrishnan, Nick Colegrave, and Peter D Keightley. Extensive de novo mutation rate variation between individuals and across the genome of *chlamydomonas reinhardtii*. *Genome Research*, 25(11):1739–1749, 2015.
- [18] J H Gillespie. *Population genetics: a concise guide*. JHU press, 2004.
- [19] Josep Díaz, Leslie Ann Goldberg, George B Mertzios, David Richerby, Maria Serna, and Paul G Spirakis. Approximating fixation probabilities in the generalized moran process. *Algorithmica*, 69(1):78–91, 2014.
- [20] Andrea Wünsche, Duy M Dinh, Rebecca S Satterwhite, Carolina Diaz Arenas, Daniel M Stoebel, and Tim F Cooper. Diminishing-returns epistasis decreases adaptability along an evolutionary trajectory. *Nature Ecology & Evolution*, 1(4):1–6, 2017.
- [21] Suman G Das, Susana OL Direito, Bartłomiej Waclaw, Rosalind J Allen, and Joachim Krug. Predictable properties of fitness landscapes induced by adaptational tradeoffs. *Elife*, 9:e55155, 2020.
- [22] Nicola Palmieri, Carolin Kosiol, and Christian Schlötterer. The life cycle of drosophila orphan genes. *elife*, 3:e01311, 2014.
- [23] Xuan Zhuang, Chun Yang, Katherine R Murphy, and C-H Christina Cheng. Molecular mechanism and history of non-sense to sense evolution of antifreeze glycoprotein gene in northern gadids. *Proceedings of the National Academy of Sciences*, 116(10):4400–4405, 2019.
- [24] Guang-An Lu, Yixin Zhao, Zhongqi Liufu, and Chung-I Wu. On the possibility of death of new genes—evidence from the deletion of de novo micrnas. *BMC genomics*, 19(1):1–8, 2018.
- [25] Chris Papadopoulos, Isabelle Callebaut, Jean-Christophe Gelly, Isabelle Hatin, Olivier Namy, Maxime Renard, Olivier Lespinet, and Anne Lopes. Intergenic orfs as elementary structural modules of de novo gene birth and protein evolution. *bioRxiv*, 2021.
- [26] Xinzhu Wei and Jianzhi Zhang. Patterns and mechanisms of diminishing returns from beneficial mutations. *Molecular biology and evolution*, 36(5):1008–1021, 2019.
- [27] Tobias JAJ Heinen, Fabian Staubach, Daniela Häming, and Diethard Tautz. Emergence of a new gene from an intergenic region. *Current biology*, 19(18):1527–1531, 2009.
- [28] Christian Schlötterer. Genes from scratch—the evolutionary fate of de novo genes. *Trends in Genetics*, 31(4):215–219, 2015.
- [29] Nikolaos Vakirlis, Omer Acar, Brian Hsu, Nelson Castilho Coelho, S Branden Van Oss, Aaron Wacholder, Kate Medetgul-Ernar, Ray W Bowman, Cameron P Hines, John Iannotta, et al. De novo emergence of adaptive membrane proteins from thymine-rich genomic sequences. *Nature communications*, 11(1):1–18, 2020.
- [30] Jorge Ruiz-Orera, Jessica Hernandez-Rodriguez, Cristina Chiva, Eduard Sabidó, Ivanela Kondova, Ronald Bontrop, Tomàs Marqués-Bonet, and M Mar Albà. Origins of de novo genes in human and chimpanzee. *PLoS genetics*, 11(12):e1005721, 2015.
- [31] Ashley Farlow, Hongan Long, Stéphanie Arnoux, Way Sung, Thomas G Doak, Magnus Nordborg, and Michael Lynch. The spontaneous mutation rate in the fission yeast *schizosaccharomyces pombe*. *Genetics*, 201(2):737–744, 2015.
- [32] Peter D Keightley, Urmi Trivedi, Marian Thomson, Fiona Oliver, Sujai Kumar, and Mark L Blaxter. Analysis of the genome sequences of three drosophila melanogaster spontaneous mutation accumulation lines. *Genome research*, 19(7):1195–1201, 2009.
- [33] Heewook Lee, Ellen Popodi, Haixu Tang, and Patricia L Foster. Rate and molecular spectrum of spontaneous mutations in the bacterium *escherichia coli* as determined by whole-genome sequencing. *Proceedings of the National Academy of Sciences*, 109(41):E2774–E2783, 2012.

- [34] Peter A Lind and Dan I Andersson. Whole-genome mutational biases in bacteria. *Proceedings of the National Academy of Sciences*, 105(46):17878–17883, 2008.
- [35] Hongan Long, David J Winter, Allan Y-C Chang, Way Sung, Steven H Wu, Mariel Balboa, Ricardo BR Azevedo, Reed A Cartwright, Michael Lynch, and Rebecca A Zufall. Low base-substitution mutation rate in the germline genome of the ciliate tetrahymena thermophila. *Genome biology and evolution*, 8(12):3629–3639, 2016.
- [36] Rob W Ness, Andrew D Morgan, Nick Colegrave, and Peter D Keightley. Estimate of the spontaneous mutation rate in chlamydomonas reinhardtii. *Genetics*, 192(4):1447–1454, 2012.
- [37] Stephan Ossowski, Korbinian Schneeberger, José Ignacio Lucas-Lledó, Norman Warthmann, Richard M Clark, Ruth G Shaw, Detlef Weigel, and Michael Lynch. The rate and molecular spectrum of spontaneous mutations in arabidopsis thaliana. *science*, 327(5961):92–94, 2010.
- [38] Gerda Saxer, Paul Havlak, Sara A Fox, Michael A Quance, Sharu Gupta, Yuriy Fofanov, Joan E Strassmann, and David C Queller. Whole genome sequencing of mutation accumulation lines reveals a low mutation rate in the social amoeba dictyostelium discoideum. *Plos One*, 2012.
- [39] Way Sung, Abraham E Tucker, Thomas G Doak, Eunjin Choi, W Kelley Thomas, and Michael Lynch. Extraordinary genome stability in the ciliate paramecium tetraurelia. *Proceedings of the National Academy of Sciences*, 109(47):19339–19344, 2012.
- [40] Yuan O Zhu, Mark L Siegal, David W Hall, and Dmitri A Petrov. Precise estimates of mutation rate and spectrum in yeast. *Proceedings of the National Academy of Sciences*, 111(22):E2310–E2318, 2014.
- [41] Donna M Cassidy-Hanley. Tetrahymena in the laboratory: strain resources, methods for culture, maintenance, and storage. *Methods in cell biology*, 109:237–276, 2012.
- [42] Ron Milo, Paul Jorgensen, Uri Moran, Griffin Weber, and Michael Springer. Bionumbers—the database of key numbers in molecular and cell biology. *Nucleic acids research*, 38(suppl\_1):D750–D753, 2010.
- [43] Janni Petersen and Paul Russell. Growth and the environment of schizosaccharomyces pombe. *Cold Spring Harbor Protocols*, 2016(3):pdb-top079764, 2016.
- [44] Elizabeth H Harris. *The Chlamydomonas Sourcebook: Introduction to Chlamydomonas and Its Laboratory Use: Volume 1*, volume 1. Academic press, 2009.
- [45] Masaki Ishida and Manabu Hori. Improved isolation method to establish axenic strains of paramecium. *Japanese Journal of Protozoology*, 50(1-2):1–14, 2017.
- [46] Petra Fey, Anthony S Kowal, Pascale Gaudet, Karen E Pilcher, and Rex L Chisholm. Protocols for growth and development of dictyostelium discoideum. *Nature protocols*, 2(6):1307–1316, 2007.
- [47] Roberta Ribeiro Silva, Célia Alencar Moraes, Josefina Bessan, and Maria Cristina Dantas Vanetti. Validation of a predictive model describing growth of salmonella in enteral feeds. *Brazilian Journal of Microbiology*, 40(1):149–154, 2009.
- [48] Miguel Angel Fernández-Moreno, Carol L Farr, Laurie S Kaguni, and Rafael Garesse. Drosophila melanogaster as a model system to study mitochondrial biology. In *Mitochondria*, pages 33–49. Springer, 2007.
- [49] Maarten Koornneef and Ben Scheres. Arabidopsis thaliana as an experimental organism. *e LS*, 2001.

## Supplementary information

Species	Generation time	Mutation rate (per base pair per generation)	Model time-step
<i>T.thermophila</i>	2 hrs	$7.6 \cdot 10^{-12}$	$3 \cdot 10^5$ yrs
<i>S.cerevisiae</i>	90 min	$1.6 \cdot 10^{-10}$	$1.1 \cdot 10^4$ yrs
<i>E.coli</i>	20 min	$2 \cdot 10^{-10}$	$1.9 \cdot 10^3$ yrs
<i>S.pombe</i>	2 hrs	$2 \cdot 10^{-10}$	$1.1 \cdot 10^4$ yrs
<i>C.reinhardtii</i>	6 hrs	$3 \cdot 10^{-10}$	$2.3 \cdot 10^4$ yrs
<i>P.tetraurelia</i>	8 hrs	$2 \cdot 10^{-11}$	$4.6 \cdot 10^5$ yrs
<i>D.discoideum</i>	4 hrs	$2.9 \cdot 10^{-11}$	$1.6 \cdot 10^5$ yrs
<i>S.typhimurium</i>	21 min	$3 \cdot 10^{-9}$	133 yrs
<i>D.melanogaster</i>	10 days	$7 \cdot 10^{-9}$	$7.8 \cdot 10^4$ yrs
<i>A.thaliana</i>	6 weeks	$9 \cdot 10^{-9}$	$2.4 \cdot 10^4$ yrs

**Fig.1–Figure Supplement 1:** Estimates of one model time-step in various species. The following references were used to obtain mutation rates: [31, 32, 33, 34, 35, 36, 37, 38, 39, 40]. And the following references were used for generation times: [41, 42, 43, 44, 45, 46, 47, 48, 49]. Most references give a range of values or multiple values of mutation rates and generation times depending on the culture conditions used. In such cases, we picked the average reported value at a single culture condition that is consistent between the studies reporting mutation rate and generation time in any one organism. The model time-step calculated in column 3 is the time it takes for 1 mutation to occur in a locus of 100 bp.

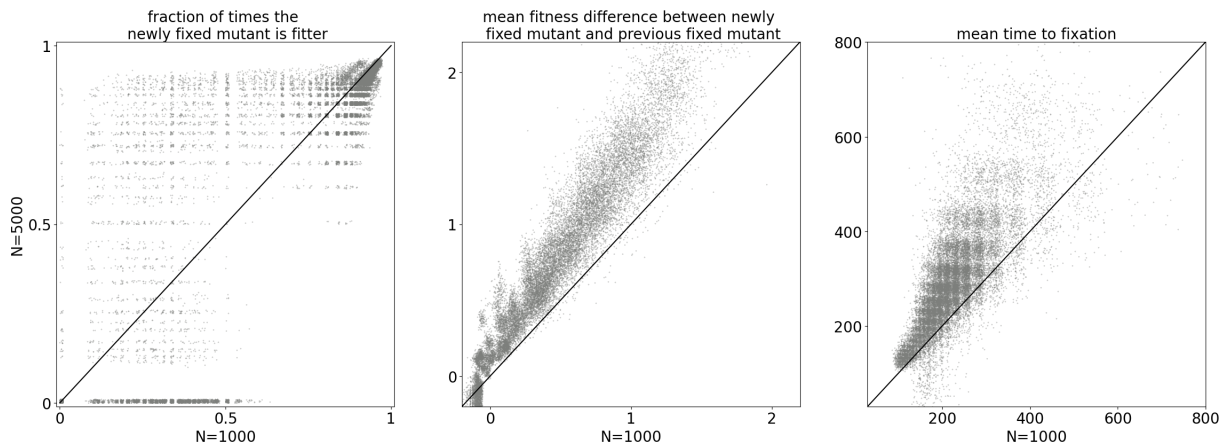


**Fig.2–Figure Supplement 1:** Scatter plots comparing fixation dynamics in N = 1000 and 5000 populations. For each population size, 22,500 systems were analysed across all parameter values. The x and y value for each point represents (A) Fraction of times fixation of fitter mutant occurred, (B) mean fitness difference between current and previous fixed mutant, (C) Mean fixation time across 2500 time steps, for an N = 1000 and an N = 5000 systems that have equal parameter values

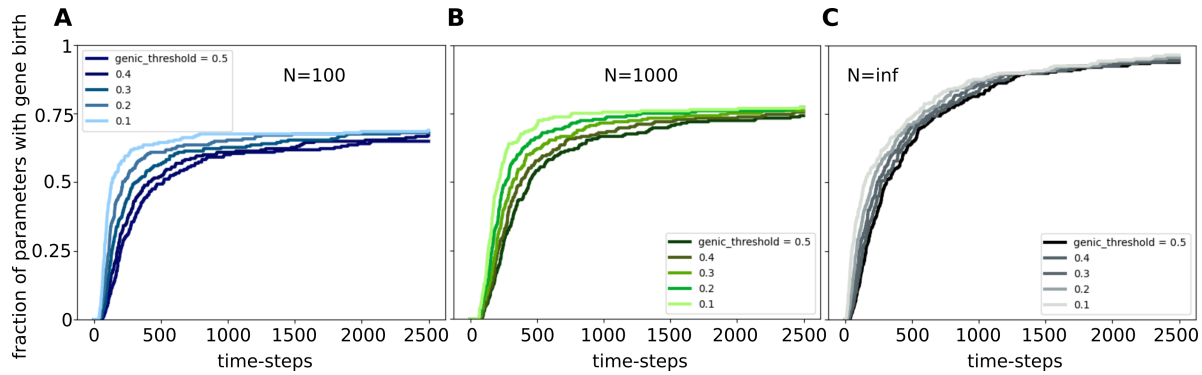


**Fig.3–Figure Supplement 1:** In (A,B,C) the x-axis represents time-steps and the y-axis represents the fraction of parameters tested for which gene birth occurred at least in 1 of the 100 replicate populations tested. Population sizes: (A)  $N=100$ , (B)  $N=1000$ , (C) infinite population.

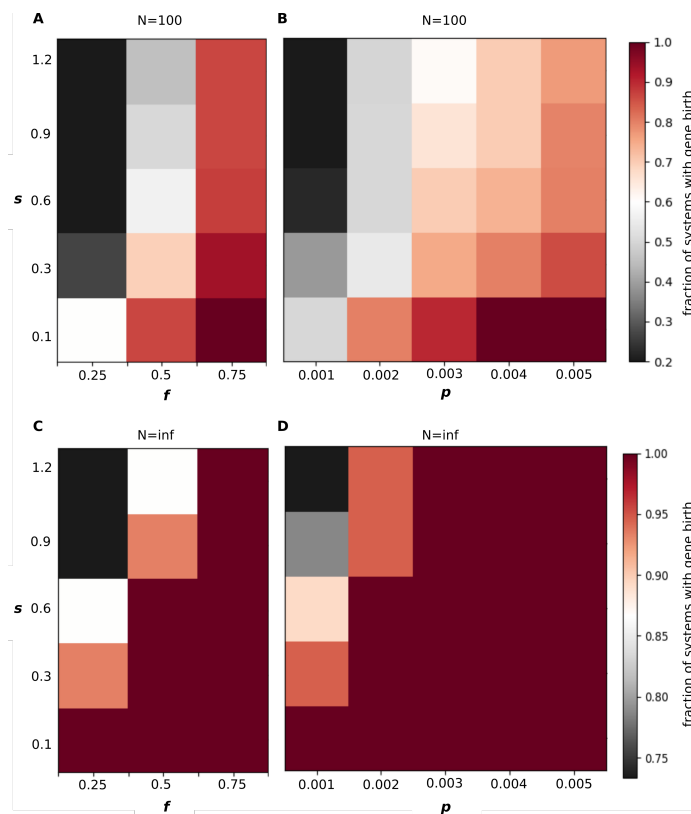


**Fig.3–Figure Supplement 2:** Trade-off between the shape parameter and frequency and size of beneficial mutations. We show results here for populations of sizes (A,B)  $N = 100$  and (C,D)  $N = \text{inf}$ . In the heatmaps of rows indicate values of the shape parameter, columns indicate values of (A,C) fraction of beneficial mutation  $f$ , (B,D) mean size of beneficial mutations  $p$ . Colors indicate the fractions of systems with gene birth as indicated by the colorbar.

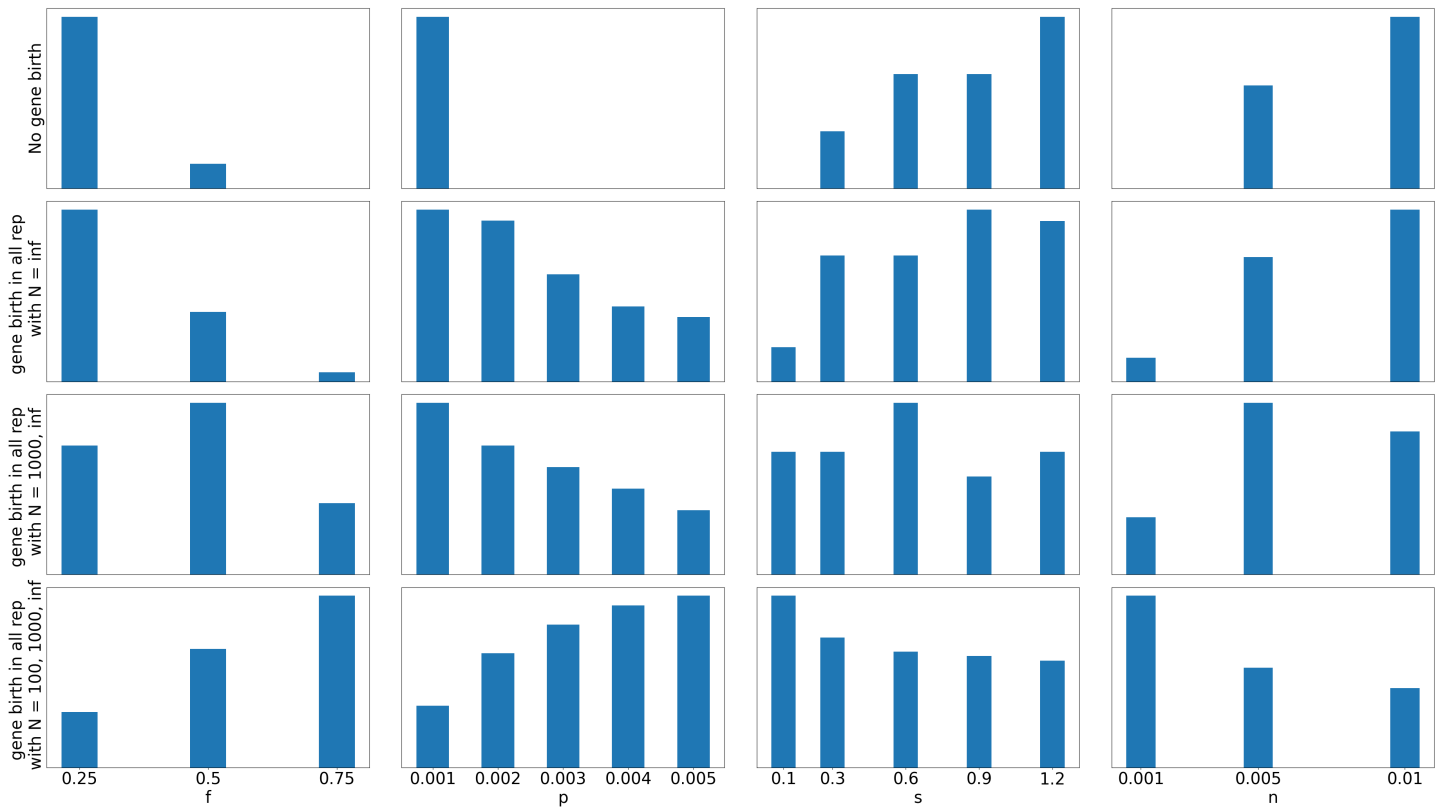


**Fig.3–Figure Supplement 3:** Effect of model parameters on gene birth probability. Each row contains histograms for parameter values at which *first row*: no gene birth occurred in any population, *second row*: gene birth occurred in all 100 replicates only in  $N = \text{inf}$  populations, *third row*: gene birth occurred in all 100 replicates only in  $N = 1000$  and  $N = \text{inf}$  populations, *fourth row*: gene birth occurred in all 100 replicates across all  $N = 100, 1000, \text{inf}$ . Columns correspond to different parameters, first column:  $f$ , second column:  $p$ , third column:  $s$ , fourth column:  $n$

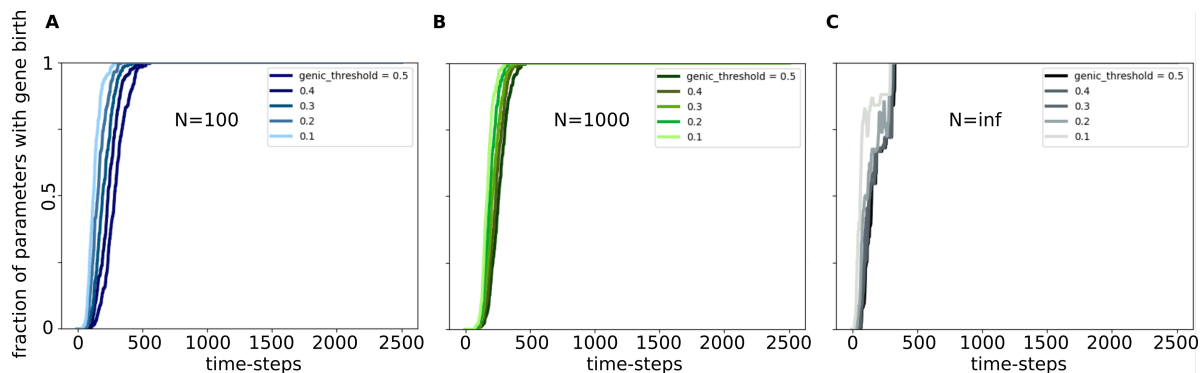


**Fig.4–Figure Supplement 1:** All parameters lead to gene birth within 2500 time-steps under the fluctuating DFE regime. In (A,B,C) the x-axis represents time-steps and the y-axis represents the fraction of parameters tested for which gene birth occurred at least in 1 of the 100 replicate populations tested. Population sizes: (A)  $N=100$ , (B)  $N=1000$ , (C) infinite population.

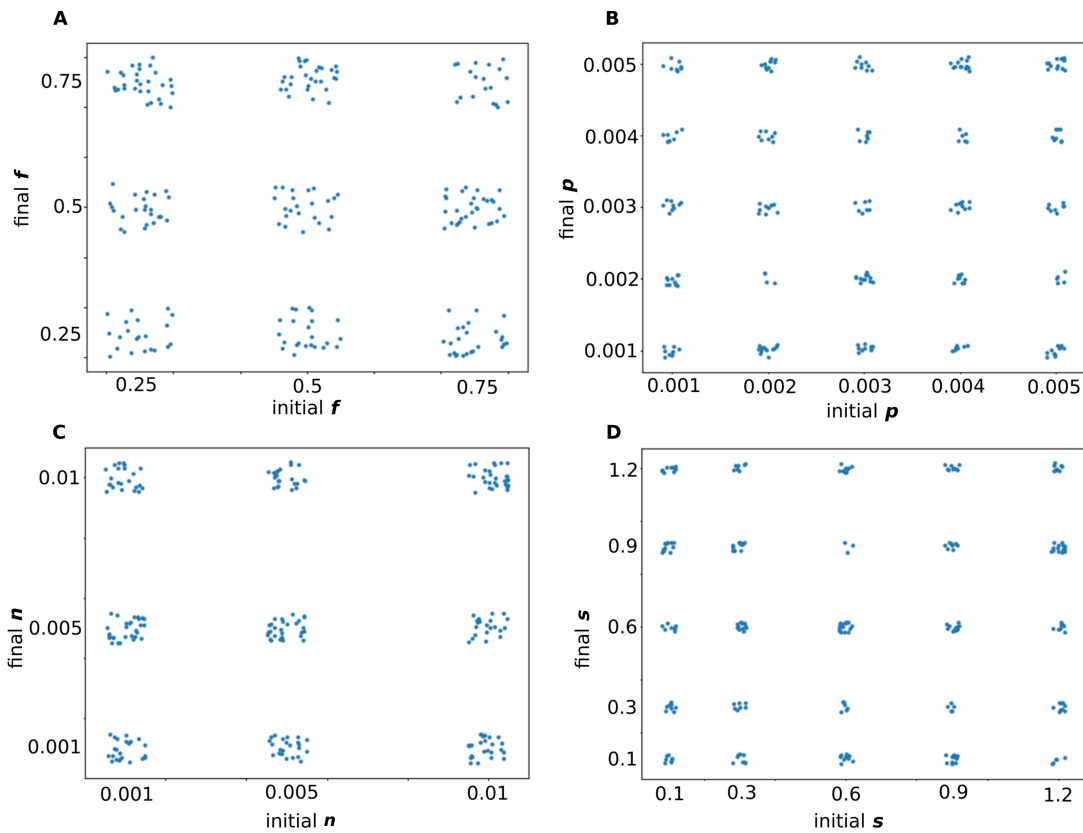


**Fig.4-Figure Supplement 2:** Scatter plots for initial and final values of parameters under fluctuating DFE regime. Each point represents a distinct  $N = 1000$  population. 2250 systems were analysed for this figure. Noise has been added to make the density of points more apparent. (A) fraction of beneficial mutations  $f$ , (B) mean size of beneficial mutations  $p$ , (C) mean size of deleterious mutations  $n$ , (D) shape parameter  $s$

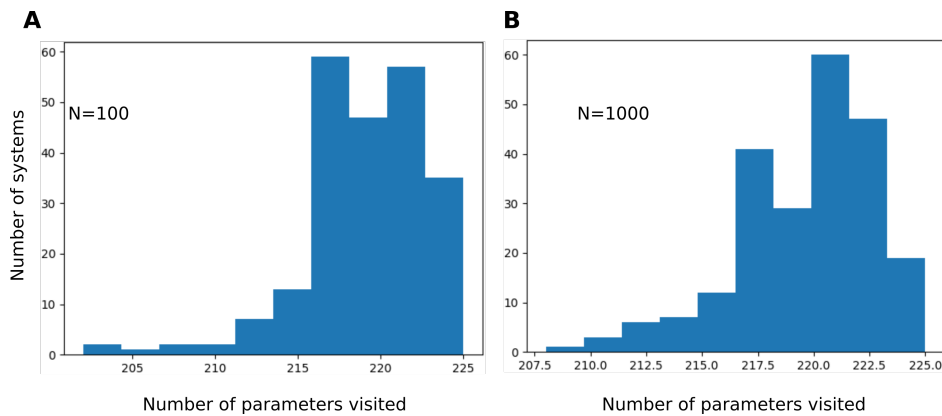


**Fig.4-Figure Supplement 3:** Histograms for number of distinct parameters visited by populations under the fluctuating DFE regime. 2250 systems were analysed for each histogram. (A)  $N = 100$ , (B)  $N = 1000$